JOURNAL OF OPTOELECTRONICS AND ADVANCED MATERIALS, Vol. 10, No. 12, December 2008, p. 3477 - 3481

Infrared and Raman spectroscopic study of Sn-containing Zn/Al-layered double hydroxides

E. M. SEFTEL[a,b*], E. POPOVICI[a], M. MERTENS[c], P. COOL[b], E. F. VANSANT[b]
[a]*Department of Physical and Theoretical Chemistry and Materials Chemistry, "Al. I. Cuza" University of Iasi, Bvd. Carol I, no 11, 700506, Romania*
[b]*Laboratory of Adsorption and Catalysis, University of Antwerpen (CDE), Universiteitsplein 1, 2610 Wilrijk, Antwerpen, Belgium*
[c]*VITO Flemish Institute for Technological Research, Boeretang 200, B-2400, Belgium*

Zn/Al- and Zn/Al/Sn-LDHs were prepared by the co-precipitation method at constant pH. The LDH structure and the local environment of the tin cations were investigated using XRD and UV-vis DR methods. Band component analysis of both infrared and Raman spectra has been used for the detailed characterization. Raman spectroscopy proved to be more useful to distinguish between the different metal-OH stretching modes than FT-IR spectroscopy. The carbonate anions were found to be in a lowered symmetry. Changes in the spectral profile were observed when part of Al^{3+} was replaced by Sn^{4+} in the brucite-like structure. The shift of a band and the appearance of a weak shoulder at 498 cm^{-1} in the Raman spectrum when the tin cations were involved indicated that small amounts of the tetravalent cations are segregated on the surface of the brucite-like sheets as very small regions of amorphous SnO_2.

(Received November 7, 2008; accepted November 27, 2008)

Keywords: layered double hydroxides; Sn-containing; isomorphic substitution; FT-IR spectroscopy; Raman spectroscopy.

1. Introduction

Layered double hydroxides (LDH), also called anionic clays having a hydrotalcite-like structure have received increased interest due to their potential applications in numerous domains, such as in green chemistry and in catalysis as precursors [1-3]. This is due to the possibility to obtain mixed metal oxides at the atomic level, rather than at a particle level throughout thermal decomposition of the layered precursor. These materials originate from the isomorphous substitution of divalent cations, such as Mg^{2+}, by trivalent cations, like Al^{3+}, in a brucite-like structure. Both Mg^{2+} and Al^{3+} can be replaced by other di- or trivalent cations giving rise to a wide variety of LDHs having the general formula $[M^{2+}_{1-x}M^{3+}_{x}(OH)_2]\cdot(A^{n-}_{x/n})\cdot mH_2O$, where M^{2+} and M^{3+} are the divalent and trivalent cations, respectively, and A^{n-} the interlayer anions [2, 3]. Some authors have studied the incorporation of tetravalent cations, such as Ti^{4+} [4], Sn^{4+} [5] or Zr^{4+} [6], into the brucite-like layers to obtain new LDHs with increased catalytic performances or to enlarge the specific surface area.

The characterization by Infrared (IR) and Raman Spectroscopy of LDHs with different M(II)-M(III) cationic pairs [7], the anionic pillaring [8] and the thermal decomposition [9] of these types of materials have been reported in the literature. Infrared spectroscopy has the disadvantage that the water in LDHs is an intense absorber, and may mask the absorbance of the MOH units. This inconvenience, however, is over fulfilled by Raman spectroscopy where the water is a very poor scatterer and the hydroxyl stretching of the MOH units may be readily observed [10].

Recent characterizations performed on the M^{IV}-containing LDHs revealed that the tetravalent cations are not all incorporated inside the layers and part of the M^{IV} atoms is segregated from the LDH phase [11]. Recently we have investigated the incorporation of Ti^{4+} in a ZnAl-LDH and we have found that approximately 50% of Ti^{4+} could be incorporated within the brucite-like sheets forming the layered structure and the other part segregated as an amorphous TiO_2 phase [12]. Velu et al. reported the possibility of incorporation of Sn^{4+} into LDH-type layers over a large composition range and claimed that up to 30% of Al^{3+} could be substituted by Sn^{4+} to form a new MgAlSn ternary LDH [13]. However, detailed spectroscopic descriptions on tetravalent substituted LDHs have not been reported. This paper focusses on the characterization of the tin containing LDHs structures using the Infrared and Raman Spectroscopic techniques followed by detailed band component analysis.

2. Experimental

Zn/Al- and Zn/Al/Sn-LDHs with the cationic ratio of 3 : 1 and 3 : 0.8 : 0.2, respectively, were prepared by the co-precipitation method at constant pH [2, 3]. The chemical composition of the final products was determined by electron probe micro analysis measurements (EPMA). X-ray diffractions were recorded on a PANalytical X'Pert PRO MPD diffractometer with filtered CuKα radiation. UV-vis-Diffuse Reflectance spectra were obtained at room temperature on a NICOLET EVOLUTION 500 UV-VIS Spectrometer, with a diffuse reflectance accessory using KBr standard white as reflectance. Diffuse Reflectance Infrared Fourier

Transform spectra (DRIFT) were measured on a Nicolet 20 DXB FTIR Spectrometer, equipped with a Spectra – Tech diffuse reflectance accessory. About 500 scans were taken with a 4 cm^{-1} resolution. For Raman spectroscopy a NICOLET NEXUS 670 instrument with a Ge detector was used. The samples were measured in a home built in situ spectroscopic cell for Fourier Transform Raman, in a 180° reflective sampling configuration using a 1064 nm Nd:YAG laser. Samples were heated at a heating rate of 5°/min under a flow of pressed air, at a flow rate of 50 cm^3/min. Band component analysis was carried out using the Peakfit software package. Lorentz-Gauss cross-product functions were used throughout and peak fitting was carried out until the squared correlation coefficients with r^2 greater than 0.995 were obtained.

3. Results

Fig. 1 displays the XRD patterns of the as-synthesized samples and they are typical of the layered double hydroxides, while their chemical compositions and the calculated unit cell parameters are summarized in table 1. The diffraction peaks are indexed in a hexagonal lattice with an R-3m rombohedral symmetry for which the unit cell parameters *a* (related with the cation-cation distance within the brucite-like sheets) and *c* (related to the thickness of the brucite-like layer and the interlayer distance) can be calculated according to $a = 2d(110)$ and $c = 3d(003)$ [3].

Table 1. Chemical compositions and structural parameters of the as-synthesized samples.

Sample	Zn/Al-LDH	Zn/Al/Sn-LDH
[1]Chemical compositions	$Zn_{0.739}Al_{0.26}(OH)_2$	$Zn_{0.711}Al_{0.23}Sn_{0.057}(OH)_2$*
a (Å)	3.06	3.07
c (Å)	23.7	23.1
d_{003} (Å)	7.9	7.7

[1]Calculated from the EPMA results (*not an indication that all the Sn^{4+} cations are within the brucite-like sheets).

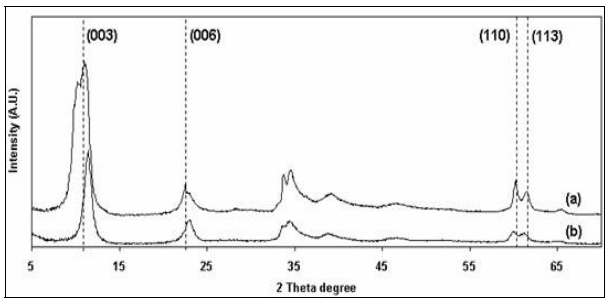

Fig. 1. The XRD patterns of (a) Zn/Al-LDH and (b) Zn/Al/Sn-LDH samples.

Diffuse reflectance UV-vis spectroscopy is a very sensitive probe for the detection of the coordination state of Sn species. The UV-vis DR spectra of the studied brucite-type solids are shown in figure 2.

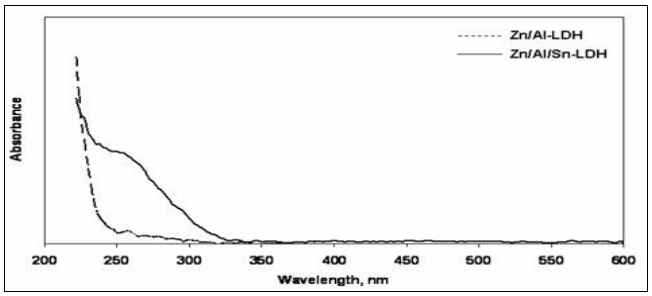

Fig. 2. The UV-vis diffuse reflectance spectra of Zn/Al-LDH and the corresponding Sn-substituted LDH solid.

Fig. 3 displays the infrared spectra of the as-synthesized Zn/Al-, Zn/Al/Sn-LDHs in the 500-4000 cm^{-1} region.

Band component analysis of the hydroxyl-stretching region shows the presence of very broad bands centered at 2944, 3291 and 3506 cm^{-1} for the Zn/Al-LDH and at 2878, 3211, 3438 and 3563 cm^{-1} for the Zn/Al/Sn-LDH sample (Fig. 4).

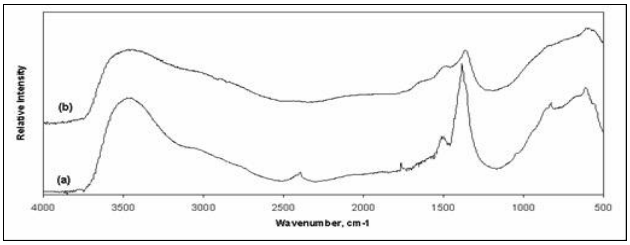

Fig. 3. FT-IR spectra of (a) Zn/Al-, and (b) Zn/Al/Sn-LDH samples in the 500-4000 cm^{-1} region.

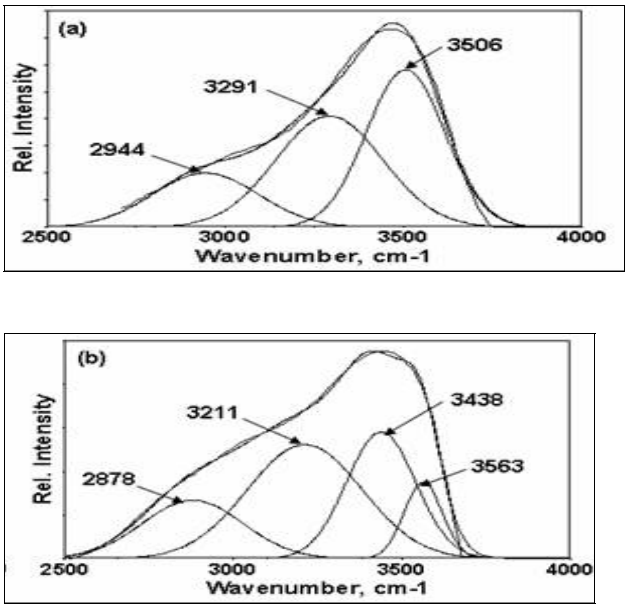

Fig. 4. Band component analysis of the FT-IR spectra of (a) Zn/Al-LDH and (b) Zn/Al/Sn/-LDH sample.

Fig. 5 illustrates the band component analysis of the 1200-1800 cm^{-1} region in the infrared spectra.

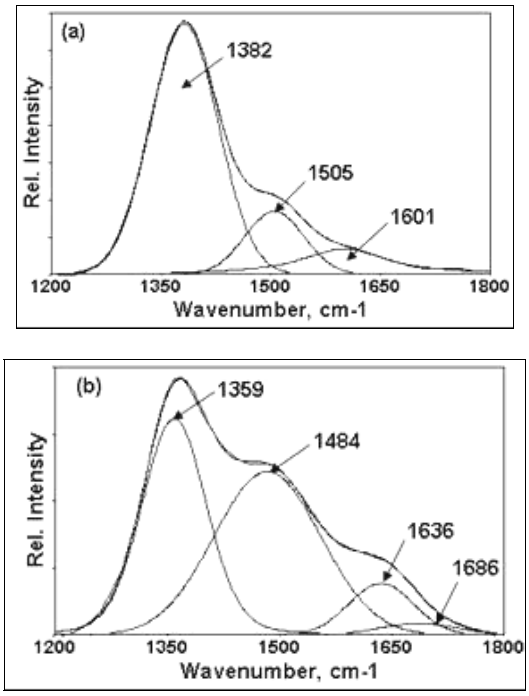

Fig. 5. Band component analysis of FT-IR spectra in the 1200-1800 cm^{-1} region for (a) Zn/Al-LDH and (b) Zn/Al/Sn-LDH sample.

Figure 6 shows the band component analysis in the low-frequency region.

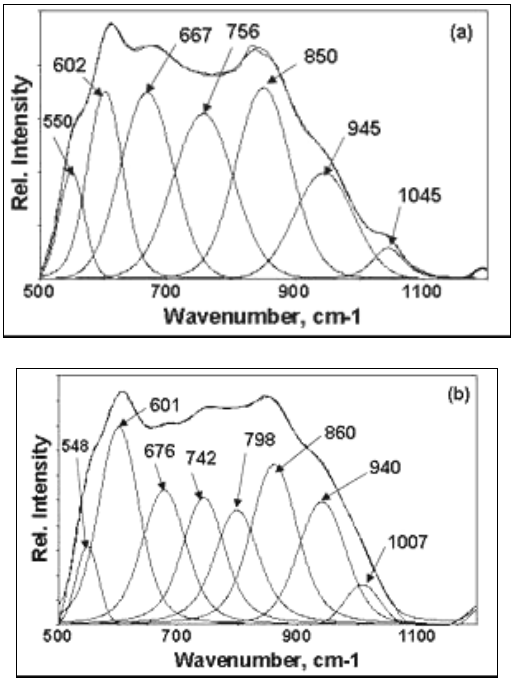

Fig. 6. Band component analysis of FT-IR spectra in the low-frequency region of (a) Zn/Al-LDH and (b) Zn/Al/Sn-LDH sample.

Fig. 7 displays the Raman spectra of the hydroxyl-stretching region for the as-synthesized samples.

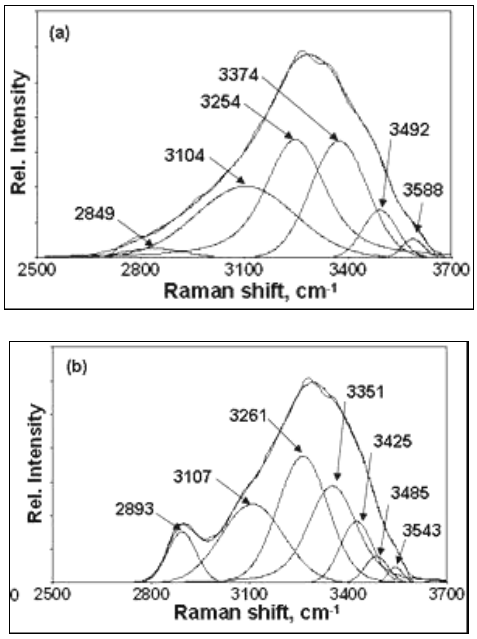

Fig. 7. Band component analysis of Raman spectra in the hydroxyl-stretching region of (a) Zn/Al- and (b) ZnAl/Sn-LDH samples.

The low frequency regions of both Zn/Al- and Zn/Al/Sn-LDH samples of the Raman spectra are shown in Figure 8.

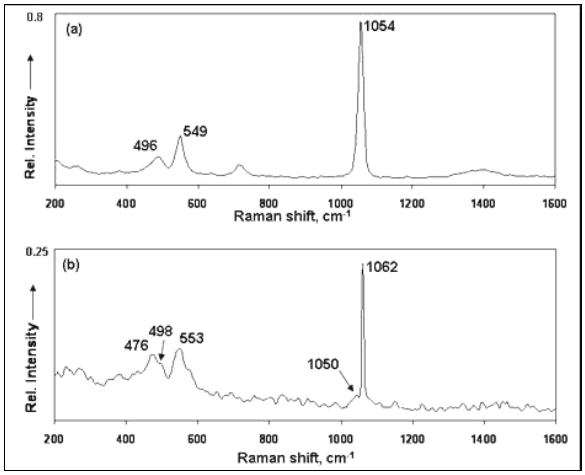

Fig. 8. Raman spectra in the low frequency region of the (a) Zn/Al-LDH and (b) Zn/Al/Sn-LDH samples.

4. Discussions

The decrease of the *c* parameter value (Table 1) for the Zn/Al/Sn-LDH sample can be attributed to the increase of the attractive force between the brucite-like sheets and the interlayer as a result of the increase of the charge density, since part of the trivalent Al^{3+} cations are isomorphously substituted by the tetravalent Sn^{4+} cations.

The increase of the *a* parameter value clearly indicates the incorporation of Sn^{4+} in the brucite-like sheets, as the ionic radius for the Sn^{4+} (0.69Å) is higher than for the Al^{3+} (0.50Å) [13].

The UV-vis DR measurements show that when the tetravalent cations are absent, a very low absorption spectrum is observed. When tin is added, two absorptions are observed at 228 nm (shoulder) and 250 nm. The shoulder observed at 228 nm can be assigned to $O^{2-} \rightarrow Sn^{4+}$ charge transfer transition of the Sn ions in a tetrahedral environment indicating the presence of Sn-O-Sn bonds as part of small SnO_2 amorphous regions. The second strong absorption corresponds to the Sn^{4+} species in an octahedral (Oh) coordination [14, 15].

The FT-IR spectra (Figure 3) show a broad intense band between 3600-3300 cm^{-1} generally assigned to the OH stretching mode of layer hydroxyl groups and the interlayer water molecules, and a weak shoulder between 2900-3100 cm^{-1} due to the OH stretching mode of the interlayer water molecules hydrogen bonded to the carbonate anions [16].

The first band observed in Figure 4 is generally attributed to the CO_3^{2-}-H_2O bridging mode [17] and the shift to lower frequencies may be attributed to the influence of the hydroxide layer composition. The second band can be assigned to the hydrogen-bonded interlayer molecules [18]. The 3400-3600 cm^{-1} region is ascribed to the metal-OH stretching modes but we cannot distinguish between the different metals (Zn, Al, Sn) bonded to the hydroxyl groups in the FT-IR spectra.

The band analysis shows that the infrared spectrum is complex in the 1200-1800 cm^{-1} region (Figure 5). The HOH bending mode of the interlayer water is observed in both spectra at 1601 and 1636 cm^{-1}. Group theoretical analysis of the unperturbed carbonate anion (D_3h symmetry) predicts four normal modes: the υ_1 symmetric stretch of *A_1'* symmetry normally observed at 1063 cm^{-1}, the υ_3 anti-symmetric stretch of *E'* symmetry observed at 1415 cm^{-1}, the υ_2 out of plane bend at 879 cm^{-1} and the in-plane bend at 680 cm^{-1}. For the unperturbed carbonate anion the υ_1 mode is Raman active only. For the perturbed carbonate anion, all modes are both Raman and IR active except for the υ_2 mode, which is IR active only [19]. The next two bands centered at 1505 and 1382 cm^{-1} for the Zn/Al-LDH, and at 1484 and 1359 cm^{-1} for the Zn/Al/Sn-LDH solids are attributed to the υ_3 anti-symmetric stretching vibrations associated with the interlayer carbonate anions. The presence of two bands in this region is an indication that the symmetry of the carbonate anions is lowered from the planar D_{3h} to the C_{2v} symmetry. As a result of this symmetry lowering the infrared inactive υ_1 mode will be activated and a weak infrared band is observed around 1000-1050 cm^{-1} [20]. The FT-IR spectrum of Sn-containing sample shows a low intensity and broad band at 1686 cm^{-1}. This band can be attributed to the presence of small amounts of water strongly coordinated to a cation which is not incorporated in the brucite-like sheets [7]. Since this broad band is not present in the Zn/Al-LDH infrared spectrum and the UV-vis DR measurements reveal the presence of some Sn^{4+} cations in a tetrahedral coordination, we may conclude that small amounts of tin are segregated on the surface of the brucite-like sheets as small regions of SnO_2 and are amorphous due to the absence of diffraction in the XRD patterns.

The low-frequency region is characterized by a complex group of seven bands (Figure 6a). The bands at 550 and 756 cm^{-1} are ascribed to the OH translation modes mainly influenced by the trivalent aluminium. The relatively broad band centered at 945 cm^{-1} is assigned to the deformation mode of the Al-OH bond in layered double hydroxides [18]. This band is shifted to 940 cm^{-1} when some aluminium cations are substituted by the tetravalent tin cations (Figure 6b). The bands observed at 602-601 cm^{-1} for the Zn/Al- and Zn/Al/Sn-LDHs solids can be interpreted as being hydroxyl translation modes influenced by the divalent cations in the brucite-like sheets. The bands observed at around 670 and 860 cm^{-1} are characteristic to the υ_4 and υ_2 modes of the interlayer carbonate anions in a lowered symmetry comparing to the unperturbed carbonate anions. The shift of the position of these modes indicates that the composition of the brucite-like sheets strongly influences the nature of the interlayer carbonate. The Zn/Al/Sn-LDH sample shows a band centered at 798 cm^{-1} which can be assigned to the vibration of oxygen bonded to the tin cations [21].

Six absorption bands are observed in hydroxyl-stretching region in the Raman spectra at 3588, 3492, 3374, 3254, 3104 and 2849 cm^{-1} for the Zn/Al-LDH sample. Taking into account the oversimplified model presented by Kloprogge et al. [19], the 3588 cm^{-1} band is attributed to the Al_3OH stretching vibration and the 3492 cm^{-1} band to the Zn_3OH stretching vibration. Different types of water vibrations can be distinguished in the region between 2500-3700 cm^{-1}, such as interlamellar water, water hydrogen bonded to the M_3OH units (where M can be Zn, Al or any combination of these metals), water which is bridged to both the M_3OH units and the carbonate anions and water bonded to the carbonate anions [19, 22]. The remaining bands in this region are attributed to OH stretching vibrations of water participating to the above described molecular environments. The 2849 cm^{-1} band, with the lowest intensity, may be attributed to vibrations of the water hydrogen bonded to the carbonate anion. The replacement of part of Al by Sn in the brucite-like structure leads to changes in the spectral profile (Figure 7b). The band assigned to the Zn_3OH units is observed at 3485 cm^{-1}. The band at 3543 cm^{-1} attributed to the Al_3OH unit is lowered in intensity and a new absorption band is observed at 3425 cm^{-1} which might be assigned to the Sn_3OH units. A significant higher intensity is observed for the 2893 cm^{-1} band indicating a greater amount of carbonate anions in the structure. The υ_1 mode of carbonate anions is observed in Figure 8 as a strong and sharp band at 1054-1062 cm^{-1}. A weak shoulder is observed at ~1050 cm^{-1} in the Zn/Al/Sn-LDH spectrum indicating two types of carbonate anions in a lowered symmetry [7]. The second most intense band in the Raman spectra appears at around 550 cm^{-1}. It is reported as being unique to the hydrotalcite-like structure [23] and has the equivalent in the infrared spectrum at 547 cm^{-1} showing

again that the symmetry of carbonate anions has been lowered from D_{3h} to C_{2v}. This band is the result of OH-O units formed when the two hydrogens of the water molecule are bridged to the two oxygen atoms of the carbonate anion. The 496 cm^{-1} band in the Zn/Al-LDH spectrum is only Raman active and can be assigned to the hydroxyl groups mainly associated with the zinc [19]. When the tetravalent cations are involved, this band is centered at 476 cm^{-1} and only a weak shoulder remains at 498 cm^{-1}. Y. Liu et al. reports a detailed analysis of the Raman spectra of the SnO_2 nanocrystallites ascribing the 476 cm^{-1} weak shoulder to the B_{2g} mode only Raman active [24] originating from the vibration mode of Sn-O bonds. Two possibilities can be considered in the present situation: (i) the band is the result of the combination of the OH groups associated with the tin cations and is strongly influenced by zinc or (ii) the presence of some Sn-O-Sn bonds as parts of some SnO_2 amorphous regions. Taking into account the informations obtained from the UV-vis DR measurements, this low intensity band is probably indicating that some Sn^{4+} cations are segregated on the surface of the brucite-like sheets as small regions of SnO_2 and are amorphous due to the absence of diffraction in the XRD patterns.

4. Conclusions

Infrared and Raman spectroscopy were used for detailed characterization of the Zn/Al- and Zn/Al/Sn-LDHs. The hydroxyl stretching units of Zn_3OH, Al_3OH and Sn_3OH were identified by unique band positions. Raman spectroscopy proved to be more effective to study the hydroxyl stretching region than infrared spectroscopy. The combination of the two techniques enables the bands ascribed to the hydroxyl units and to the water molecules to be distinguished. A very low intensity and broad band at 1686 cm^{-1} in the FT-IR spectrum of the Sn-containing sample indicated the presence of small amounts of water strongly coordinated to a cation which is not incorporated in the brucite-like sheets. The shift of a band position in the Raman spectrum of the Sn-containing LDH supported the possibility of segregation of small amounts of tin cations on the surface of the brucite-like sheets which could not be detected by X-ray diffraction method.

Acknowledgments

This study was supported by the NoE project "Inside Pores" and the GOA project funded by the Special Fund for Research of the University of Antwerp. This work is also part of the CEEX No. 1/S1/2005 project.

References

[1] Y. Guo, D. Li, C. Hu, E. Wang, Y. Zou, H. Ding, S. Feng, Micropor. Mesopor. Mater. **56,** 153 (2002).
[2] F. Cavani, F. Trifiro, A. Vaccari, Catal. Today **11**, 201 (1991).
[3] S. M. Auerbache, K. A. Carrado, P. K. Dutta, Handbook of layered materials, Marcel Dekker, Inc., New York (2004).
[4] N. Das, A. Samal, Micropor. Mesopor. Mater. **72**, 219 (2004).
[5] M. P. Kapoor, Y. Matsumura, Catal. Today, **93-95**, 287 (2004).
[6] C. Jiménes-Sanchidrián, J. M. Hidalgo, R. Llamas, J. R. Ruiz, Appl. Catal., A **312,** 86 (2006).
[7] J. T. Kloprogge, R. L. Frost, J. Solid State Chem. **146**, 506 (1999).
[8] R. L. Frost, A. W. Musumeci, J. Bouzaid, M. O. Adebajo, W. N. Martens, J. T. Kloprogge, J. Solid State Chem. **178**, 1940 (2005).
[9] R. L. Frost, A. W. Musumeci, T. Bostrom, M. O. Adebajo, M. L. Weier, W. Martens, Themochim. Acta **429,** 179, (2005).
[10] R. L. Frost, A. W. Musumeci, W. N. Martens, M. O. Adebajo, J. Bouzaid, J. Raman Spectrosc. **36**, 925, (2005).
[11] M. Intissar, F. Malherbe, V. Prévot, F. Leroux, J. Colloid Interface Sci. **299,** 747, (2006).
[12] E. M. Seftel. E. Popovici, M. Mertens, G. Van Tendeloo, P. Cool, E. F. Vansant, Micropor. Mesopor. Mater. **111**, 12, (2008).
[13] S. Velu, K. Suzuki, T. Osaka, F. Ohashi, S. Tomura, Mater. Res. Bull. **34**, 1707, (1999).
[14] G. Luo, S. Yan, M. Qiao, K. Fan, Appl. Catal., A **332**, 79, (2007).
[15] P. Shah, A. V. Ramaswamy, K. Lazar, V. Ramaswamy, Micropor. Mesopor. Mater. **100,** 210, (2007).
[16] G. Carja, R. Nakamura, T. Aida, H. Niiyama, Micropor. Mesopor. Mater. **47**, 275, (2001).
[17] R. L. Frost, K. L. Erikson, Spectrochim. Acta, Part A **60**, 3001, (2004).
[18] J. T. Kloprogge, L. Hickey, R. L. Frost, J. Raman Spectrosc. **35**, 967, (2004).
[19] T. E. Johnson, W. Martens, R. L. Frost, Z. Ding, T. T. Kloprogge, J. Raman Spectrosc. **33,** 604, (2002).
[20] J. T. Kloprogge, D. Wharton, L. Hickey, R. L. Frost, Am. Mineral. **87,** 623, (2002).
[21] C. A. Moina, G. O. Ybarra, J. Electroanal. Chem. **504**, 175, (2001).
[22] R. L. Frost, K. L. Erickson, Spectrochim. Acta, Part A **61,** 2697, (2005).
[23] R. L. Frost, B. J. Reddy, Spectrochim. Acta, Part A **65**, 553, (2006).
[24] Y. Liu, et al., Colloids Surf., A (2007), doi: 10.1016/j.colsurfa.2007.06.054.

*Corresponding author: seftel_elena@yahoo.com